On the minimisation of resource utilisation for cost reduction in space division multiplexing based elastic optical networks

Sridhar Iyer

Department of Electronics and Communication Engineering,
S.G. Balekundri Institute of Technology,
Nehru Nagar, Shivabasava Nagar, Belagavi,
Karnataka 590010, India
Email: sridhariyer1983@gmail.com

Abstract: In the current work, for a Space Division Multiplexing (SDM) based Elastic Optical Network (EON) (SDM-b-EON), a routing, modulation format, spatial granularity (*SpGl*), and spectrum assignment (RMFSpGlSA) problem is formulated with an aim to minimise the overall network cost by reducing the resource usage. RMFSpGlSA is formulated as a joint integer linear program (J-ILP) model (J-ILP-RMFSpGlSA), and the ILP-RMFSpGl+SA model which successively solves the RMFSpGl and the SA problems. Extensive simulations are conducted to evaluate the performances of the two formulated ILP models with an aim to find the 'best' *SpGl* value under various conditions. The obtained results demonstrate that fine values of *SpGl* are mostly chosen with the widening of guardband width values, and with an increase in the mean bit-rate values of demands, a coarse value of *SpGl* is mostly chosen. Finally, all the results demonstrate that ILP-RMFSpGl+SA obtains similar performance when compared to J-ILP-RMFSpGlSA simultaneously requiring much lesser execution times.

Keywords: elastic optical networks; space division multiplexing; ILP; switching; resource allocation.

Reference to this paper should be made as follows: Iyer, S. (2022) 'On the minimisation of resource utilisation for cost reduction in space division multiplexing based elastic optical networks', *Int. J. Internet Protocol Technology*, Vol. 15, No. 1, pp.29–40.

Biographical notes: Sridhar Iyer received the BE degree in Electronics and Telecommunications Engineering from Mumbai University, India in 2005. He received the MS degree in Electrical and Communication Engineering from New Mexico State University, USA in 2008, and the PhD degree from Delhi University, India in 2017. Currently he is an Associate Professor in the Department of ECE, S.G. Balekundri Institute of Technology, India. His research interests include the architectural, algorithmic, and performance aspects of the optical networks, with current emphasis on efficient design and resource optimisation in the space division multiplexing enabled flexi-grid Elastic optical networks. He has published over 60 peer-reviewed articles in the aforementioned areas.

1 Introduction

The Elastic Optical Networks (EONs) provide flexibility in the spectrum via frequency slots (FSs) by using the spectral super-channel switching method that forms the super-channels which combine the sub-carriers such that their transmission, routing and reception occurs in the form of a single lightpath (Iyer, 2020). The main characteristics of EONs include the (i) application of different modulation formats (MFs) differing in both, spectral-efficiency (SE) and transmission reach, (ii) employment of signal regeneration execution ability with modulation conversion and spectrum conversion, and (iii) transmission of super-channel(s) (Iyer, 2020a). Further, over the network, transmission of a high capacity super-channel may comprise of multiple optical carriers which are generated or terminated utilising the transceiver(s) that use a specific MF, and carry a part of the total traffic. The basic EON optimisation problem of routing and spectrum allocation (RSA) is known to be NP-hard (Iyer, 2019). Further, if the MF(s) choice is also included, RSA transforms into the RMFSA problem which must account for the (i) *Spectrum contiguity constraint*, (ii) *Spectrum continuity constraint*, and (iii) *MF decision* (Iyer, 2019). To improve the spectral-efficiency, the EONs satisfy the Nyquist condition which requires the guardbands (GuBds) only between the successive spectral super-channels and not between the sub-carriers (Jinno, 2017; Iyer, 2018).

In recent years, it has been envisioned that even with deployment of the EONs, the capacity crunch will persist since the EONs use only two *multiplexing* dimensions which in turn limit their throughput by the fibre capacity (Klinkowski et al., 2018). To provision the exponentially growing capacity for the future diverse Internet traffic, compared to the EONs, the Space Division Multiplexing (SDM) based EONs (SDM-b-EONs) use various compatible fibre which increase their capacity to much higher magnitudes (Saridis et al., 2015; Klinkowski et al., 2018; Pandya et al., 2020; Pandya et al., 2020a). In the SDM-b-EONs, with 'space' (i.e., core, mode or fibre) as an added dimension, it may be required to opt for the spatial super-channel switching method in which, over the same component of the spectrum, the sub-carriers are placed across multiple or all the dimensions of space (*DoS*) of the chosen fibre solution (Klinkowski et al., 2018). Further, in the spatial super-channel case, on one hand, the sub-carriers occurring at the same frequency in multiple *DoS* share one Laser source (Winzer and Neilson, 2017); on the other hand, there is a requirement of GuBds on every *DoS* of a spatial super-channel. As an extension, it may also be required to consider the spatial spectral super-channel switching method in which, multiple spectral super-channels are placed in the same component of the spectrum which extends over multiple *DoS* (Xia et al., 2015). Hence, if *su* and *sp* represent the contiguous sub-carriers and *DoS* within the same spectrum component, respectively then, a $su \times sp$ spatial spectral super-channel is a hybrid of a $su \times 1$ spectral-super-channel and a $1 \times sp$ spatial-super-channel.

In the SDM-b-EONs, the switching architectures provisioning flexibility in both, the space and the spectrum can increase the network capability (Klinkowski et al., 2018). Further, the physical layer impairments (Pandya et al., 2014; Pandya et al., 2014a) introduced by a particular fibre solution has a direct impact on the adopted switching method which in turn is a major factor that determines the architecture and the properties of the optical switches deployed at the various nodes of a SDM-b-EON (Marom et al., 2017; Ho et al., 2014). The three main switching methods applicable to any SDM-b-EON are: (i) Flexi-grid and Flexi-space switching (FGFSS), (ii) Flexi-grid Set space switching (FG-SSS), and (iii) Group Flexi-grid Set space switching (G-FG-SSS) (Marom and Blau, 2015). FGFSS provides the utmost flexibility; however, compared to the other methods, it needs the largest amounts of wavelength selective switches (WSSs) (Klonidis et al., 2015). FG-SSS presents limitations on the spectrum flexibility; however, it requires the least WSSs amounts (Klonidis et al., 2015). G-FG-SSS splits all the spatial dimensions set into multiple groups (*GP*) of spatial dimension which are subsets of the *DoS* (Khodashenas et al., 2017). Further, assuming uniform grouping; G-FG-SSS sets the spatial granularity $(SpGl)$ value that indicates the $DoS's$ level of grouping, equal to $|GP|$. Also, from G-FG-SSS, FGFSS and FG-SSS can be obtained i.e., $SpGl = 1$ and $SpGl = |DoS|$ correspond to FGFSS and FG-SSS, respectively.

The SDM-b-EONs need to deploy the WSS compatible with the adopted switching method (Shariati et al., 2017). Further, the choice of a particular WSS is also dependent on the manner in which the operation of both, a network node and network node degree of a reconfigurable optical add/drop multiplexer (ROADM) occurs which implies whether the constraint of continuity in 'space' is to be met, or if it is to be relaxed which results in more flexibility in the switching however, leading to more WSS port amounts (Moreno-Muro et al., 2017). The authors in (Khodashenas et al., 2017; Shariati et al., 2017) have demonstrated that the WSSs use is significantly affected by the *SpGl* value. Further, there exists a direct relation of *SpGl* with the super-channels since, the chosen *SpGl* value is used to determine the *DoS* amount in a *GP* (Klinkowski et al., 2018). This is consequence of the fact that there is a direct relation between *SpGl* and the three main switching methods wherein, *DoS* which a super-channel occupies equals the *DoS* amount in a *GP* (Klinkowski et al., 2018)]. Further, it is also known that the highest and the lowest spectral-efficiency is obtained by the spectral super-channels and the spatial super-channels, respectively (Rumipamba-Zambrano et al., 2018). However, in terms of the required Lasers amount, the opposite is true i.e., the spectral super-channels and the spatial super-channels need the lowest and the highest amount of Lasers, respectively (Rumipamba-Zambrano et al., 2018). The study conducted by (Rumipamba-Zambrano et al., 2018) has also demonstrated that the spatial spectral super-channels obtain balanced values of the network resources (i.e., FS, WSS, and Laser).

Many studies in literature have investigated the issue of resource assignment in the spectrally and spatially flexible SDM-b-EONs (Klonidis et al., 2015; Khodashenas et al., 2017; Shariati et al., 2017; Moreno-Muro et al., 2017; Rumipamba-Zambrano et al., 2018; Iyer, 2020b; Rottondi, 2017). However, on one hand, in few of these studies, for the SDM-b-EON performance evaluation, impact of varying *SpGl* values has not been considered, on the other hand, in few of these studies, even though the performance evaluations have been conducted considering varying *SpGl* values, it is assumed that the *SpGl* value is known a-priori. With *SpGl* value being set by the adopted switching method in a SDM-b-EON, the *SpGl* value has a major effect on the overall network cost since; a fine *SpGl* consumes lesser spectral resources as lesser guard bands are required whereas, when *SpGl* is set with a coarse value, major reduction in the usage of other resources viz., WSSs and Lasers, can be obtained. Hence, in view of the aforementioned, as a major contribution, in this work; we formulate a routing, modulation format (MF), SpGl, and spectrum assignment (RMFSpGlSA) problem with an aim to minimise the overall network cost by reducing the resource use in a SDM-b-EON. Unlike existing studies, we

obtain solutions to the formulated problem for finding the 'best' SpGl value under various conditions. Initially, we formulate the RMFSpGlSA problem as joint ILP (J-ILP) model, named as J-ILP-RMFSpGlSA. Next, to obtain better convergence and reasonable execution times, we split J-ILP-RMFSpGlSA as the RMFSpGl+SA problem, named as ILP-RMFSpGl+SA, which successively solves the RMFSpGl and the SA problem.

The following point must be noted regarding our current study: we have chosen a route enabled ILP model since, compared to a link enabled model, a route enabled ILP model is more efficient as it minimises the amount of variables needed for decision making and also, it inherently satisfies the spectrum-continuity constraint (Klinkowski et al., 2018). Also, to the best of the author's knowledge, the current work is the first which formulates the RMFSpGlSA problem and simultaneously conducts extensive simulations with an aim to decide on the 'best' SpGl value in a SDM-b-EON design. The rest of the paper is structured as follows: In Section 2, we formulate the J-ILP-RMFSpGlSA problem. Section 3 details the formulation of the ILP-RMFSpGl+SA problem. In Section 4, we present the simulation results. Finally, Section 5 concludes the study.

2 Formulation of the J-ILP-RMFSPGLSA problem

In this section we detail the formulation of the J-ILP-RMFSpGlSA problem for which, initially, we define the various notations and the variables and decision variables following which, we detail the objective function and the various considered constraints.

2.1 Notations

In this sub-section, we define the various notations which are used in the current study.

- A graph $G(V,E)$ which represents a network topology graph. In $G(V,E)$, V and E denote the nodes and the links set, respectively. Within the network, the aggregate degree of the nodes is denoted as $DE_{aggregate}$. Further, the demands set is denoted as D which consists of the various demands d, and for each demand d, the candidate routes are denoted as R_d.
- MF_r denotes the largest level of the MF which is used over $r \in R_d$. It must be noted that the MF_r value is dependent on the transmission reach and is obtained from the studies by (Shariati et al., 2017; Rumipamba-Zambrano et al., 2018). Further, for all the network links, the dimensions of space set is denoted as DoS.
- The DoS groups GP set is denoted as $\psi : \psi = \bigcup_{SpGl \in K} \xi_{SpGl}$ where, the DoS groups GP set of $SpGl$ is denoted as ξ_{SpGl}. Under the assumption of uniform grouping, every DoS group GP belonging to ξ_{SpGl} consists of $SpGl$ DoS which implies that $SpGl = |GP|$. Lastly, the available $SpGl$ set is denoted as $K : K = \{1, ..., SpGl, ..., |DoS|\}$. It must be noted that K consists of different amount of elements depending on the fibre solution which is adopted. For e.g. if MMF is used then, $K : SpGl = \{|DoS|\}$; however, if MCF is used then, the $SpGl$ value is an integer multiple of the $SpGl$ amount that appear in groups.
- The required FSs amount including the GuBds is denoted as fs^d_{rGP} considering every DoS in GP and provided that the DoS in GP and the route r are chosen for the provisioning of a demand d. Further, the fs^d_{rGP} value is evaluated using the study by (Jinno, 2017).
- The required lasers amount for a demand d is denoted as la^d_{rGP} considering that a DoS in GP and the route r are chosen for the provisioning of a demand d. Further, with the consideration of the MF_r value, the la^d_{rGP} value is evaluated using the study by (Klinkowski et al., 2018).
- The large positive upper bound values of the network resources i.e., WSSs, lasers and FSs is denoted as $T_{WSS}, T_{Laser}, and\ T_{FS}$, respectively.
- To provide the option of setting the importance value to a network resource, $\eta, \xi, and\ \lambda$ are used which denote the related cost of the WSSs, lasers and FSs, respectively.

2.2 Variables and decision variables

In In this sub-section, we define all the integer variables $\in Z^+$ and the decision variables $\in \{0,1\}$ which are used to formulate the J-ILP-RMFSpGlSA problem.

- The variable $FS_{\max}$ which denotes the required FSs largest index within the SDM-b-EON.
- The variable $WSS_{\max}$ which denotes the aggregate required WSSs amount within the SDM-b-EON.
- The variable $LASER_{\max}$ which denotes the aggregate required lasers amount within the SDM-b-EON.
- The variable FS^{start}_d which denotes, for a demand d, the start of the FS index.
- The variable $laser_d$ which denotes, for provisioning a demand d, the required lasers amount.
- The decision variable $\Delta^{d\,d'} = 1$ when the last FS index of d' is lesser than FS^{start}_d; else, $\Delta^{d\,d'} = 0$.

- The decision variable $\Omega_{SpGl}=1$ when, for provisioning the demands, $SpGl$ is chosen as the 'best' $SpGl$ value; else, $\Omega_{SpGl}=0$.
- The decision variable $y_{rGP}^{d}=1$ when, for provisioning a demand d, the routes $r's$ DoS in GP is chosen; else, $y_{rGP}^{d}=0$. Further, $y_{rGP}^{d}=1$ implies that a demand $d's$ last FS index $FS_d^{last}=FS_d^{start}+fs_{rGP}^{d}$.

2.3 Objective function and considered constraints

With the various defined notations and variables, the objective function of the J-ILP-RMFSpGlSA problem is:

$$Minimise \quad \lambda\cdot FS_{\max}+\xi\cdot WSS_{\max}+\eta\cdot LASER_{\max} \tag{1}$$

From (1), it can be seen that aim of J-ILP-RMFSpGlSA is to reduce the overall network cost by minimising the usage of the various network resources. The objective function in (1) is subjected by the following constraints:

- The constraint in (2) guarantees that, to provision demands, only '1' $SpGl$ $SpGl\in K$ can be chosen.

$$\sum_{SpGl\in K}\Omega_{SpGl}=1 \tag{2}$$

- The FS constraint in (3) guarantees that for any $d\in D$, $FS_{\max}$ is not lesser than value of FS_d^{last}.

$$FS_{\max}\geq FS_d^{start}+fs_{rGP}^{d}\cdot y_{rGP}^{d}\ \forall d\in D, r\in R_d, GP\in\psi \tag{3}$$

- The WSS constraint in (4) is adopted from the studied by (Khodashenas et al., 2017; Shariati et al., 2017) and is used to evaluate the WSSs amount for every degree. Hence, (4) ensures that when (i) $\Omega_{SpGl}=1$, $WSS_{\max}\geq 2\cdot DE_{aggregate}\cdot\left|DoS\right|/SpGl$, and (ii) $\Omega_{SpGl}=0$, owing to the presence of the T_{WSS} value on the LHS, (4) does not hold.

$$T_{WSS}\cdot\left(1-\Omega_{SpGl}\right)+WSS_{\max}\geq 2\cdot DE_{aggregate}\cdot\left|DoS\right|/SpGl \quad \forall SpGl\in K \tag{4}$$

- For every $d\in D$, the Lasers constraint in (5a) when (i) $\Omega_{SpGl}=1$, $laser_d\geq la_{rGP}^{d}$, and (ii) $\Omega_{SpGl}=0$, owing to presence of the T_{Laser} value on the LHS, (5a) does not hold. Consequently, (5b) guarantees that $LASER_{\max}$ exceeds the aggregate of the required Lasers amount.

$$T_{Laser}\cdot\left(1-y_{rGP}^{d}\right)+laser_d\geq la_{rGP}^{d} \quad \forall d\in D, r\in R_d, GP\in\psi \tag{5a}$$

$$LASER_{\max}\geq\sum_{d\in D}laser_d \tag{5b}$$

- The routing constraint in (6) guarantees that every $d\in D$ is assigned with a unique lightpath. Specifically, for every $d\in D$, (6) ensures that when (i) $\Omega_{SpGl}=1$, to provision a demand d, only a single combined value of GP and r can be chosen which implies an aggregate value of '1', and (ii) $\Omega_{SpGl}=0$, the aggregate value equals '0'.

$$\sum_{r\in R_d}\sum_{GP\in\xi_{SpGl}}y_{rGP}^{d}\quad\forall d\in D, SpGl\in K \tag{6}$$

- The spectrum-contiguity constraint in (7) ensures that either $\Delta^{dd'}$ or $\Delta^{d'd}$ can have a value equal to '1'.

$$\Delta^{dd'}+\Delta^{d'd}=1\quad\forall d,d'\in D: d\neq d' \tag{7}$$

- The non-overlapping constraint in (8) ensures that the same GP is used for the transmission of two demands d and d' if their corresponding chosen lightpaths r and r', respectively have links which are joint. The aforementioned scenario occurs when $y_{rGP}^{d}=1$, $y_{r'GP}^{d'}=1$, and $r\cap r'\neq\Theta$. Further, since (7) ensures that either $\Delta^{dd'}$ or $\Delta^{d'd}$ can have a value equal to '1', for (8), there occur the following two cases: (i) if $\Delta^{dd'}=1$, then, following the $\Delta^{dd'}$ definition, $FS_d^{start}\geq FS_{d'}^{start}+fs_{r'GP}^{d'}$, and (ii) if $\Delta^{d'd}=0$, owing to presence of T_{FS} on the RHS, (8) does not hold.

$$FS_d^{start}\geq FS_{d'}^{start}+fs_{r'GP}^{d'}-T_{FS}\cdot\left[\left(y_{rGP}^{d}+y_{r'GP}^{d'}+\Delta^{dd'}\right)\right] \quad \forall d,d'\in D, r\in R_d, r'\in R_{d'}, GP\in\psi: d\neq d', r\cap r'\neq\Theta \tag{8}$$

- The spectrum-continuity constraint is inherently satisfied by J-ILP-RMFSpGlSA since, a route enabled ILP model has been chosen for the formulation (Klinkowski et al., 2018).

It must be noted that J-ILP-RMFSpGlSA has limitations in the convergence owing mainly to the spectrum-contiguity and the spectrum-continuity constraints. Hence, to improve the convergence and to obtain the solutions in reasonable execution times, we formulate the ILP- RMFSpGl+SA problem in the next section.

3 Formulation of the ILP-RMFSpGl+SA problem

The formulation of the ILP-RMFSpGl+SA problem is conducted in two phases. In the first phase, the formulation finds the $SpGl$ value and sets the MFs for all the demands assuming the relaxation of the spectrum-continuity constraint. In the next phase, the formulation allocates the

FSs to the demands considering the output obtained from the first phase and ensuring that the spectrum continuity constraint is satisfied. To formulate the ILP-RMFSpGl+SA problem, for the two phases, we detail the various notations, the variables, the objective function and the various considered constraints.

3.1 Formulation of the ILP-RMFSpGl problem

The notations which are applicable to the ILP-RMFSpGl problem are those which were used to formulate J-ILP-RMFSpGlSA (*see sub-section 2.1*). Further, all the variables defined for J-ILP-RMFSpGlSA are also applicable (*see sub-section 2.2*) to ILP-RMFSpGl. However, in ILP-RMFSpGl, there is relaxation of spectrum-continuity constraint and hence, variables related to spectrum i.e., $FS_{\max}$, FS_d^{start}, and $\Delta^{dd'}$ are not applicable. Also, ILP-RMFSpGl requires the definition of another integer variable $\in Z^+$, $FS_{l\arg est}$ which denotes the largest FSs amounts utilised in every *DoS* over all the network links. With the various notations and variables, ILP-RMFSpGl objective is:

$$Minimise \quad \lambda \cdot FS_{l\arg est} + \xi \cdot WSS_{\max} + \eta \cdot LASER_{\max} \tag{9}$$

The comparison of (1) and (9) shows similarities except the fact that, unlike J-ILP-RMFSpGlSA, owing to relaxation of the spectrum continuity constraint, ILP-RMFSpGl only accounts for the FSs amounts utilised irrespective of the manner in which these FSs are allocated. Finally, the objective function in (9) is subjected to all the constraints defined for J-ILP-RMFSpGlSA except constraints associated to spectrum which are defined in (3), (7) and (8). Further, for $FS_{l\arg est}$, the constraint in (10) is required which ensures that, over a link e, for the demands which pass through GP, considering $GP \in \psi$ over every link $e \in E$, $FS_{l\arg est}$ value must always exceed aggregate required FSs.

$$FS_{l\arg est} \geq \sum_{d \in D} \sum_{r \in R_d : e \in r} y_{rGP}^d \cdot fs_{rGP}^d \quad \forall GP \in \psi, e \in E \tag{10}$$

Next, in addition to the notations applicable to ILP-RMFSpGl, owing to the fact that ILP-SA is dependent on the outputs of ILP-RMFSpGl, two additional notations are required to be defined for the ILP-SA formulation.

- To provision the demands, the *SpGl* value which is required is denoted as $SpGl_{output} : SpGl_{output} = \left\{ SpGl \in K \left| \Omega_{SpGl} = 1 \right. \right\}$.
- To provision a demand *d*, the lightpath which is allocated and the *DoS* group are denoted as r_{output}^d and GP_{output}^d, respectively. Further, $r_{output}^d, GP_{output}^d : r_{output}^d, GP_{output}^d = \left\{ r \in R_d, GP \in \psi \left| y_{rGP}^d = 1 \right. \right\}$.

The variables related to the spectrum i.e., $FS_{\max}$, FS_d^{start}, and $\Delta^{dd'}$, which were not included in ILP-RMFSpGl are required to be considered for ILP-SA formulation since the spectrum-continuity constraint is required to be satisfied. With all notations and variables, objective function of the ILP-SA problem is given as follows:

$$Minimize \quad \lambda \cdot FS_{\max} + \xi \cdot WSS_{\max} + \eta \cdot LASER_{\max} \tag{11}$$

It can be observed from (11) that the objective function of ILP-SA is same as that of J-ILP-RMFSpGlSA (see (1)). However, the following two points must be considered: (i) from ILP-RMFSpGl, *SpGl* value $\left(SpGl_{output}\right)$ is already obtained and hence, following the dependence of $WSS_{\max}$ on only *SpGl* value, $WSS_{\max}$ value is a constant, and (ii) from ILP-RMFSpGl, values of $SpGl_{output}$, r_{output}^d and GP_{output}^d are already obtained and hence, value of N_{su} is a constant owing to the fact that BR_d has a fixed value and BR_{su} depends on chosen lightpath's length. Therefore, the $LASER_{\max}$ value is a constant. Considering the aforementioned two points, (11) can be simplified as follows:

$$Minimise \quad FS_{\max} \tag{12}$$

From (12) it can be inferred that the aim of ILP-SA is to reduce the required FSs maximum index within the network simultaneously ensuring that every demand is allocated the FSs under consideration of spectrum continuity constraint.

Finally, as first constraint, $FS_{l\arg est}$ value, which is also lower bound value of $FS_{\max}$ and which is found by relaxing spectrum continuity constraint, is defined in (13) to obtain better convergence from ILP-SA. Further, objective function in (12) is also subjected to the three constraints associated with spectrum which were not considered in ILP-RMFSpGl. However, it must be noted that *SpGl* value and MFs are already determined by ILP-RMFSpGl and hence, spectrum related constraints in (14), (15) and (16) are the simplified versions of the corresponding constraints in (3), (7) and (8).

$$FS_{\max} \geq FS_{l\arg est} \tag{13}$$

$$FS_{\max} \geq FS_d^{start} + fs_{r_{output}^d GP_{output}^d}^d \quad \forall d \in D \tag{14}$$

$$\Delta^{dd'} + \Delta^{d'd} = 1 \quad \forall d, d' \in D : d \neq d' \tag{15}$$

$$\begin{aligned} FS_d^{start} &\geq FS_{d'}^{start} + fs_{r_{output}^{d'} GP_{output}^{d'}}^{d'} - T_{FS} \cdot \left(1 - \Delta^{dd'}\right) \\ &\forall d, d' \in D : d \neq d', \\ &r_{output}^d \cap r_{output}^{d'} \neq \Theta, GP_{output}^d = GP_{output}^{d'} \end{aligned} \tag{16}$$

In regard to the complexity of the formulated ILP problems, the maximum values of the dominant variables and the constraints is (i) $\max\left\{O\left(\left|D\right|^2\right), O\left(k \cdot \left|D\right| \cdot \left|DoS\right|\right)\right\}$ and $O\left(k^2 \cdot \left|D\right|^2 \cdot \left|DoS\right|\right)$ for J-ILP-RMFSpGlSA, where k

denotes the candidate routes which are chosen for a demand d, (ii) $O\left(k\cdot|D|\cdot|DoS|\right)$ for ILP-RMFSpGl, and (iii) $O\left(|D|^2\right)$ for ILP-SA.

4 Simulation results and discussions

In this section, we compare the performance of the two proposed ILP models with the existing k-shortest path (k-SP) and the first-fit SA (FF-SA) algorithms, named as k-SP-FF-SA (Christodoulopoulos et al., 2011). To find solutions from the ILP models, we use the CPLEX optimisation software (IBM ILOG CPLEX optimizer, 2020). Further, for determining the candidate paths for every source-destination nodes pairs, we use the k-shortest path algorithm with a fixed value of k = 3 which has been shown to demonstrate the best performance in the SDM-b-EONs (Parello et al., 2016). In regard to the k-SP-FF-SA method, in all the cases, we obtain the results after 3000 iterations. For the performance evaluations, we consider two realistic network topologies, the small distance Deutsche Telekom (DT), and the larger distance GEANT, as shown in Figure 1. The details of the two topologies including the various dimensions values can be found in the author's previous studies (Iyer, 2020; Iyer, 2018; Iyer 2020a).

As already mentioned, for the network modelling, we assume the spectrum to be split into 12.5 GHz FSs and the transceivers to function at a fixed baud-rate 32 Gbaud with the transmission or reception of a sub-carrier occurring through a transceiver which occupies 37.5 GHz (Rottondi et al., 2017). Further, to minimise the filtering effect at the network nodes, and to split two demands, a 6.25 GHz GuBd is assigned on either end of the DoS which is already occupied. Finally, the BRs which are supported by a transceiver are according to the spectral-efficiency of a specific MF, and the transmission reaches of the considered MFs are MFs are adopted from the studies by (Shariati et al., 2017; Rumipamba-Zambrano et al., 2018).

4.1 Performance evaluations for various optimisation aims

In this sub-section, for both the considered network topologies, we present the performance evaluation results considering various optimisation aims for which we re-write equation (1) as:

$$\begin{aligned} Minimise\ \ & \lambda\cdot FS_{\max}+\xi\cdot WSS_{\max}+\eta\cdot LASER_{\max} \\ & =\lambda\cdot\left(FS_{\max}+\frac{\xi}{\lambda}\cdot WSS_{\max}+\frac{\eta}{\lambda}\cdot LASER_{\max}\right) \end{aligned} \tag{17}$$

Further, equation (17) can be equivalently re-written as:

$$\begin{aligned} Minimise\ \lambda\cdot & \left(FS_{\max}+\frac{\xi}{\lambda}\cdot WSS_{\max}+\frac{\eta}{\lambda}\cdot LASER_{\max}\right) \\ & =FS_{\max}+\sigma_{WSS:FS}\cdot WSS_{\max} \\ & +\sigma_{LASER:FS}\cdot LASER_{\max} \end{aligned} \tag{18}$$

where $\sigma_{WSS:FS}$ and $\sigma_{LASER:FS}$ denote the unit cost ratio of the WSSs and the FSs and the lasers and the FSs, respectively.

Figure 1 The network topologies considered in the simulations: (a) DT, and (b) GEANT

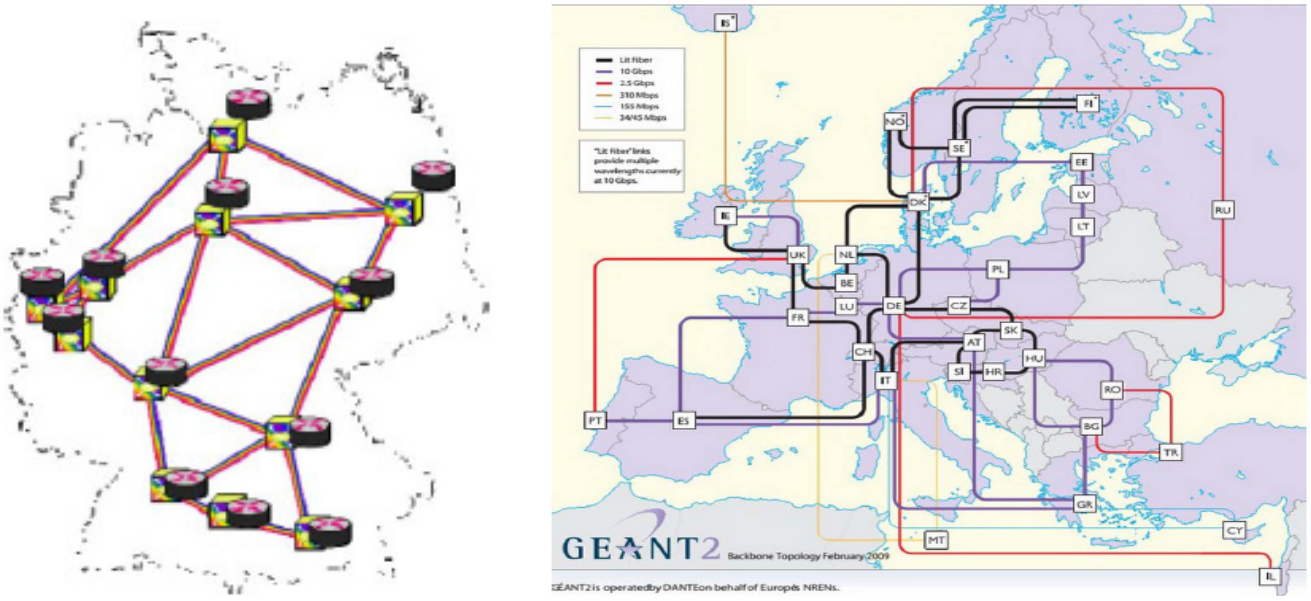

(a) (b)

With the definition of the aforementioned resources cost ratios, we evaluate and compare the performances of the two formulated ILP models with the *k*-SP-FF-SA method considering both the network topologies. To present the obtained results, we define the following: (i) the amounts of the FSs, the WSSs and the lasers are denoted as $N \cdot FSs$, $N \cdot WSSs$ and $N \cdot LASERs$, respectively, (ii) for $D \in D_{new}$, $N \cdot SpGl$ denotes the amount of times a particular $SpGl$ value has been selected as the 'best' $SpGl$ value, (iii) the amount of times that ILP-RMFSpGl+SA and *k*-SP-FF-SA select the 'best' $SpGl$ value is denoted as $N \cdot Same$, (iv) $COST$ denotes the objective function of equation (20), (v) GAP denotes the mean gap (in %) between the J-ILP-RMFSpGlSA $COST$ value and that obtained by ILP-RMFSpGl+SA and *k*-SP-FF-SA, and (vi) $Runtime$ (in seconds) denotes the time it takes by every method for the execution to obtain the solutions.

Initially, we present the results which are obtained when the DT network is considered for the simulation experiments. In this set of experiments, as the fibre solution, we assume the use of independent SMFs bundle based MuFs with 12 bundles that follows a granularity of '2' i.e. $SpGl = \{2,4,6,8,10,12\}$. Further, the case of uniform grouping $(SpGl = |GP|)$ is considered in the experiments. We stochastically generate 50 varied demands matrices which compile a new demands set D_{new}, and for every matrix of the demands, between every source-destination nodes pairs, we assume the existence of 'one' demand d which is unidirectional. Following the study by (Khodashenas et al., 2017), the demands' BRs are assumed to be distributed normally with a mean value of 3000 Gbps and a deviation of 300 Gbps. Finally, we consider the D_{new} value for every $\sigma_{WSS:FS}$ and $\sigma_{LASER:FS}$ combinations with a variation in the values of $\sigma_{WSS:FS}$ and $\sigma_{LASER:FS}$ between 0.01 - 1.

The obtained results for different optimisation aims considering the DT network topology for J-ILP-RMFSpGlSA, and ILP-RMFSpGl+SA and k-SP-FF-SA are presented in Tables 1 and 2, respectively. From the two tables it can be observed that in regard to the choice of 'best' $SpGl$ value, various combinations of $\sigma_{WSS:FS}$ and $\sigma_{LASER:FS}$ result in various decisions.

Specifically, from Table 1 it can be seen that when $\sigma_{WSS:FS}$ or $\sigma_{LASER:FS}$ has lesser values such as $\sigma_{WSS:FS}, \sigma_{LASER:FS} = 0.01$ then, compared to the WSSs and the Lasers, there occurs more preservation of the spectrum. Consequently, a fine $SpGl$ value such as $SpGl = 8$ is chosen more number of times compared to a coarse $SpGl$ value such as $SpGl = 10 \; or \; 12$. However, the coarsest $SpGl$ value of $SpGl = 12$ is always chosen for higher values of $\sigma_{WSS:FS}$ and $\sigma_{LASER:FS}$ i.e., when $\sigma_{WSS:FS}, \sigma_{LASER:FS} = 1$. Further, it can also be observed from the table that even for the lesser values of $\sigma_{WSS:FS}$ and $\sigma_{LASER:FS}$, the values of $SpGl = 2,4,6$ are never chosen; however, the higher $SpGl$ values such as $SpGl = 12$ is still chosen. The aforementioned is a consequence of the fact that on one hand, a fine $SpGl$ value minimises the GuBds amount between the super-channels on the other hand, within the chosen GP, it results in larger contiguous FSs being required which in turn increases the $FS_{\max}$ value when multiple demands are provisioned based on the sharing of the same GP over the same link. Therefore, a fine $SpGl$ value mostly minimises the FSs utilisation owing to the GuBds minimisation whereas; a coarse $SpGl$ value may not always minimise the FSs utilisation. Hence, it can be inferred that when the values of $\sigma_{WSS:FS}$ and $\sigma_{LASER:FS}$ is high such as $\sigma_{WSS:FS}, \sigma_{LASER:FS} \approx 1$, for provisioning the demands, FG-SSS is the most appropriate switching method. Lastly, it can also be observed that as $\sigma_{WSS:FS}$ and $\sigma_{LASER:FS}$ change from a lower to a higher value, there is no significant effect on the FSs which are required; however, the WSSs and the lasers amount are seen to minimise significantly which implies that a fine $SpGl$ value may not always be the 'best' value even when the FSs amount exceeds the WSSs and the lasers amount.

Table 1 The performance evaluation results for different optimisation aims considering J-ILP-RMFSpGlSA and the DT network topology

Resources Cost Ratio		*J-ILP-RMFSpGlSA*										
$\sigma_{WSS:FS}$	$\sigma_{LASER:FS}$	$N \cdot FSs$	$N \cdot WSSs$	$N \cdot LASERs$	$N \cdot SpGl$						*Cost*	*Runtime (sec)*
					2	*4*	*6*	*8*	*10*	*12*		
0.01	0.01	18.4	90.2	112.3	0	0	0	25	9	16	18.224	6.2
	0.05	18.4	90.2	112.2	0	0	0	25	9	16	19.721	8.5
	0.1	20.6	35.4	112.2	0	0	0	25	9	16	19.982	24.5
	0.5	20.6	35.4	53.7	0	0	0	0	6	44	23.774	55.9
0.05	0.01	18.4	90.2	112.3	0	0	0	25	9	16	19.832	6.4
	0.05	18.4	90.2	112.2	0	0	0	25	9	16	20.231	10.2
	0.1	20.6	35.4	112.2	0	0	0	25	9	16	21.942	32.2
	0.5	20.6	35.4	53.7	0	0	0	0	6	44	24.653	59.5

Table 1 The performance evaluation results for different optimisation aims considering J-ILP-RMFSpGlSA and the DT network topology (continued)

Resources Cost Ratio		*J-ILP-RMFSpGlSA*										
$\sigma_{WSS:FS}$	$\sigma_{LASER:FS}$	$N \cdot FSs$	$N \cdot WSSs$	$N \cdot LASERs$	$N \cdot SpGl$						*Cost*	*Runtime (sec)*
					2	*4*	*6*	*8*	*10*	*12*		
0.1	0.01	18.4	90.2	112.3	0	0	0	25	9	16	19.932	8.2
	0.05	18.4	90.2	112.2	0	0	0	25	9	16	20.873	14.7
	0.1	20.8	35.4	112.2	0	0	0	25	9	16	22.341	38.6
	0.5	20.8	34.0	53.1	0	0	0	0	4	46	26.363	50.6
0.5	0.01	20.8	35.4	53.7	0	0	0	0	6	44	21.832	7.5
	0.05	20.8	35.4	53.7	0	0	0	0	6	44	22.954	12.3
	0.1	20.8	35.4	53.7	0	0	0	0	6	44	24.021	30.2
	0.5	21.0	33.8	51.3	0	0	0	0	0	50	28.762	32.7
1	≤ 1	18.4	32	47.6	0	0	0	0	0	50	-	≤ 6.8
≤ 1	1	18.4	32	47.6	0	0	0	0	0	50	-	≤ 83.7

Table 2 The performance evaluation results for different optimisation aims considering ILP-RMFSpGl+SA and k-SP-FF-SA, and the DT network topology

Resources Cost Ratio		*ILP-RMFSpGl+SA*			*k-SP-FF-SA*		
$\sigma_{WSS:FS}$	$\sigma_{LASER:FS}$	$N \cdot Same$	$GAP(\%)$	$Runtime(\sec)$	$N \cdot Same$	$GAP(\%)$	*Runtime (sec)*
0.01	0.01	100	0	1.1	88	0.6	12.3
	0.05	100	0	1.4	87	0.7	12.3
	0.1	100	0	3.8	88	0.9	12.3
	0.5	100	0	6.7	96	1.6	12.3
0.05	0.01	100	0	1.1	86	0.7	12.3
	0.05	100	0	1.6	85	1.0	12.3
	0.1	100	0	4.1	90	0.9	12.3
	0.5	100	0	5.8	94	2.7	12.3
0.1	0.01	100	0	1.2	85	1.0	12.3
	0.05	100	0	2.2	89	0.7	12.3
	0.1	100	0	5.1	84	1.0	12.3
	0.5	100	0	6.0	96	2.7	12.3
0.5	0.01	100	0	0.5	86	2.0	12.3
	0.05	100	0	1.6	85	1.9	12.3
	0.1	100	0	1.8	85	2.0	12.3
	0.5	100	0	1.9	100	1.0	12.3
1	≤ 1	100	0	≤ 0.7	100	$0.6 \sim 1.1$	< 11.2
≤ 1	1	100	0	≤ 5.6	100	$0.5 \sim 1.1$	< 11.2

Next, comparing Table 1 and Table 2 shows that ILP-RMFSpGl+SA obtains similar performance when compared to J-ILP-RMFSpGlSA. Specifically, ILP-RMFSpGl+SA can be observed to require much lesser execution times to obtain a 0% GAP value and $N \cdot Same = 100$. For the aforementioned reason, in Table 2 the $SpGl$ related details (i.e, $N \cdot FSs$, $N \cdot WSSs$, and $N \cdot LASERs$) for ILP-RMFSpGl+SA is not presented as it is the same as that for J-ILP-RMFSpGlSA. Lastly, it can also be observed that the *k*-SP-FF-SA method obtains worst results when compared to the two formulated ILP models with the times of execution the highest as the results are obtained after 3000 iterations.

Next, we present the results which are obtained when the GEANT network is considered for the simulation experiments. In this set of experiments, as the fibre solution, we assume the use of independent SMFs bundle based MuFs with 18 bundles that follows a granularity of '2' i.e. $SpGl = \{2,4,6,8,10,12,14,16,18\}$. Further, the case of uniform grouping $(SpGl = |GP|)$ is considered in the experiments. We stochastically generate 20 varied demands matrices which compile a new demands set D_{new}, and for every matrix of demands, between every source-destination nodes pairs, we assume the existence of 'one' demand d

which is unidirectional. Similar to the DT network case, the demands' BRs are assumed to be distributed normally with a mean value of 3000 Gbps and a deviation of 300 Gbps. Finally, we consider the D_{new} value for every $\sigma_{WSS:FS}$ and $\sigma_{LASER:FS}$ combinations with a variation in the values of $\sigma_{WSS:FS}$ and $\sigma_{LASER:FS}$ between 0.001 - 0.1.

The obtained results for different optimisation aims considering the GEANT network topology for ILP-RMFSpGl+SA and *k*-SP-FF-SA are presented in Tables 3 and 4, respectively. Owing to the fact that GEANT is a large distance network, J-ILP-RMFSpGlSA is not able to generate efficient results within reasonable execution times which implies that the optimal solutions cannot be generated in the GEANT network case. Therefore, in the tables, we are unable to present the $N \cdot Same$ and the *GAP* results. To obtain the results presented in Table 3, the ILP-RMFSpGl and the ILP-SA are run for a maximum of 2 hours (7200 seconds) and 10 minutes (600 seconds), respectively. Further, since ILP-RMFSpGl provides the lower bound results when compared to the J-ILP-RMFSpGlSA results, we show the *Lower Bound* values in Table 3. Finally, in Table 3, the $Runtime = 7200^{*}$ value implies that for all the stochastically generated 20 varied demands matrices, the execution time of the ILP-RMFSpGl or the ILP-SA has atleast once reached the maximum bounded runtime of 7200 seconds or 600 seconds, respectively.

It can be observed from the two tables that the results obtained considering the GEANT network follow a similar trend to those which were obtained when the DT network was considered. Specifically, for lesser values of $\sigma_{WSS:FS}$ or $\sigma_{LASER:FS}$ such as $\sigma_{WSS:FS}, \sigma_{LASER:FS} = 0.001$, in comparison to the WSSs and the Lasers, spectrum is more preserved which leads to fine values of *SpGl* being chosen more number of times compared to a coarse *SpGl* value. However, coarsest *SpGl* values are chosen most often for higher values of $\sigma_{WSS:FS}$ and $\sigma_{LASER:FS}$ with $SpGl = 18$ being always chosen for $\sigma_{WSS:FS}, \sigma_{LASER:FS} = 0.1$. Further, it can be clearly seen that ILP-RMFSpGl+SA obtains much better results compared to *k*-SP-FF-SA.

Table 3 The performance evaluation results for different optimisation aims considering ILP-RMFSpGl+SA, and the GEANT network topology

Resources Cost Ratio		*ILP-RMFSpGl+SA*													
		ILP-RMFSpGl			*ILP-SA*		$N \cdot SpGl$								
$\sigma_{WSS:FS}$	$\sigma_{LASER:FS}$	*Lower Bound*	*COST*	*Runtime (sec)*	*COST*	*Runtime (sec)*	*2*	*4*	*6*	*8*	*10*	*12*	*14*	*16*	*18*
0.001	0.001	48.756	53.436	7200*	55.872	3.2	8	4	3	2	2	1	0	0	0
	0.005	49.872	55.589	7200*	60.452	1.0	8	4	2	3	2	1	0	0	0
	0.01	51.238	56.451	7200*	58.874	30.5*	7	3	2	2	4	2	0	0	0
	0.05	63.987	64.871	7200*	66.641	289.7*	2	2	5	6	5	0	0	0	0
	0.1	72.651	73.983	7200*	74.973	445.1*	0	0	3	7	10	0	0	0	0
0.005	0.001	51.842	57.350	7200*	60.998	21.0	1	0	0	8	4	3	2	2	0
	0.005	53.451	58.332	7200*	59.334	217.6*	0	1	0	8	4	2	3	2	0
	0.01	55.298	59.834	7200*	62.233	5.8	0	0	2	7	3	2	2	4	0
	0.05	65.921	67.983	7200*	68.452	312.8*	0	0	0	2	2	5	6	5	0
	0.1	74.381	76.554	7200*	77.354	315.7*	0	0	0	0	0	3	7	5	5
0.01	0.001	56.766	60.003	7200*	63.233	18.3	0	0	0	0	6	8	4	1	1
	0.005	56.929	61.934	7200*	62.224	187.3*	0	0	0	0	6	8	4	1	1
	0.01	58.438	62.336	7200*	63.793	257.3*	0	0	0	0	6	7	3	2	2
	0.05	68.832	69.883	7200*	70.092	408.3*	0	0	0	0	1	2	2	5	10
	0.1	76.543	77.765	7200*	79.833	487.1*	0	0	0	0	0	0	1	7	12
0.05	0.001	67.922	79.832	7200*	80.332	547.8*	0	0	0	0	0	0	3	7	10
	0.005	71.833	80.043	7200*	81.112	549.8*	00	0	0	0	0	0	3	7	10
	0.01	74.563	81.224	7200*	81.598	552.3*	0	0	0	0	0	0	2	8	10
	0.05	79.988	83.981	7200*	85.945	600*	0	0	0	0	0	0	0	0	20
	0.1	86.562	86.785	7200*	90.342	600*	0	0	0	0	0	0	0	0	20
0.1	0.001	82.345	91.223	7200*	93.487	600*	0	0	00	0	0	0	0	0	20
	0.005	76.951	92.998	7200*	94.487	600*	0	0	0	0	0	0	0	0	20
	0.01	82.376	93.278	7200*	94.687	600*	0	0	0	0	0	0	0	0	20
	0.05	94.998	95.439	7200*	97.623	600*	0	0	0	0	0	0	0	0	20
	0.1	99.988	99.032	7200*	99.879	578.9*	0	0		0	0	0	0	0	

Table 4 The performance evaluation results for different optimisation aims considering *k*-SP-FF-SA, and the GEANT network topology

Resources Cost Ratio		*k-SP-FF-SA*	
$\sigma_{WSS:FS}$	$\sigma_{LASER:FS}$	*COST*	*Runtime (sec)*
0.001	0.001	70.334	670.6
	0.005	71.651	670.9
	0.01	74.879	670.4
	0.05	85.291	669.7
	0.1	94.381	669.0
0.005	0.001	73.981	669.5
	0.005	75.472	669.8
	0.01	76.582	669.5
	0.05	86.920	669.4
	0.1	95.176	668.9
0.01	0.001	77.734	669.3
	0.005	79.271	669.6
	0.01	79.980	669.2
	0.05	89.925	669.7
	0.1	97.682	669.2
0.05	0.001	98.286	669.7
	0.005	98.679	669.4
	0.01	99.102	669.5
	0.05	103.287	669.0
	0.1	108.540	669.5
0.1	0.001	111.286	670.3
	0.005	112.897	669.4
	0.01	113.476	669.8
	0.05	115.453	669.0
	0.1	119.893	668.6

Finally, in Table 5, for ILP-RMFSpGl+SA we show the mean resources amount which are incurred when $\sigma_{WSS:FS}$ and $\sigma_{LASER:FS}$ are set to 0.001 and 0.1 which implies that fine *SpGl* values and coarse *SpGl* values are chosen mostly, respectively. It can be observed from the table that the coarse *SpGl* value does not have a major effect on the required FSs amount; however, it significantly impacts the required WSSs and Lasers amount. Therefore, only when equal importance is imposed on the requirement of all the resources, a coarse *SpGl* value is the 'best' value.

Table 5 The mean FSs, WSSs, and Lasers amount for the lowest and highest resources cost ratio

Resources Cost Ratio		*ILP-RMFSpGl+SA*		
$\sigma_{WSS:FS}$	$\sigma_{LASER:FS}$	$N \cdot FS$	$N \cdot WSSs$	$N \cdot LASERs$
0.001	0.001	54.3	364.2	854.8
0.1	0.1	68.3	80.1	226.8

4.2 Performance evaluation considering varying guard-band width and demands size

In this sub-section, we evaluate the manner in which the GuBd width effects the determination of the 'best' *SpGl* value. The motivation behind such an analysis is that there occurs a trade-off when a fine value of *SpGl* is chosen i.e. on one hand such a value minimises the GuBds amount which occur in the *SPs* which are occupied between successive super-channels; on the other hand, it results in the requirement of larger WSSs and lasers amounts. Therefore, it can be inferred that a fine value of *SpGl* is more advantageous for wider GuBds whereas, a coarse *SpGl* value is beneficial for the GuBds which are narrow in turn resulting is a minimisation of the WSSs and lasers amounts.

We consider the DT network and the same stochastically generated 50 varied demands matrices (D_{new}) for the performance evaluations since considering the GEANT network does not provide the optimal solutions. Also, we set $\sigma_{WSS:FS}, \sigma_{LASER:FS} = 0.01$ since it encompasses the different *SpGl* values. Lastly, the GuBd values are varied starting from the 6.25 GHz value to a maximum value of 50 with a granularity of 6.25 GHz.

Table 6 Effect of the GuBd width on the determination of the 'best' *SpGl* value

GuBd Width (GHz)	*J-ILP-RMFSpGlSA*						*ILP-RMFSpGl+SA*	
	$N \cdot SpGl$							
	2	*4*	*6*	*8*	*10*	*12*	$N \cdot Same$	*GAP (%)*
6.25	0	0	0	25	9	16	100	0
12.50	0	0	0	25	9	16	100	0
18.75	0	0	0	30	9	11	100	0
25.00	0	0	0	30	9	11	100	0
31.25	0	0	0	35	7	8	100	0
37.50	0	0	0	40	6	4	100	0
43.75	0	0	0	45	3	2	100	0
50.00	0	0	0	50	0	0	100	0

The obtained results are shown in Table 6 from which it can be observed that the fine values of *SpGl* are mostly chosen with the widening of the GuBd width values. Also, for a GuBd width value of 50 GHz, $SpGl = 8$ is only chosen. Further, compared to the optimal solution obtained by J-ILP-RMFSpGlSA, ILP-RMFSpGl+SA is observed to provide the same results since $N \cdot Same = 100$ and $GAP(\%) = 0$ is obtained for all the GuBd values. Overall, the results shown in Table 6 follow the trends which can be inferred from the analysis of the theory.

Further, intuitively, by fixing the GuBd value, a fine value of *SpG*l must be suitable for the small size demands consisting matrices within D_{new}. Hence, as an extension to the above results which were obtained with a variation in the GuBd width, in the next set of experiments, we fix the GuBd width. Also, since the same D_{new} value must be used as in the previous experiments, we vary the following ratio: $\mu = FSs\ for\ transmission / FSs\ used\ by\ GuBd$.

For the simulation experiments, we consider the DT network with a fixed value of $\sigma_{WSS:FS}, \sigma_{LASER:FS} = 0.01$.

Also, from D_{new}, we consider 20 new sets in which, every demand's size is varied in the range between 0.5-3 times of the corresponding one in D_{new}, respectively. Thus, in the new demands set, the mean BR for every demand falls within the range of 1500–9000 Gbps.

The obtained results are shown in Table 7 from which it can be observed that with an increase in the mean BR values of the demands, a coarse value of *SpGl* is mostly chosen which occurs owing to the fact that in the simulations, irrespective of the increase in the demands sizes or the decrease in the GuBd values, μ is increased. It can also be observed that in this case also, ILP-RMFSpGl+SA provides similar results to those provided by J-ILP-RMFSpGlSA.

Table 7 Effect of the demands size on the determination of the 'best' *SpGl* value

Mean BR of the demand (Gbps)	*J-ILP-RMFSpGlSA*						*ILP-RMFSpGl+SA*	
	N · SpGl							
	2	*4*	*6*	*8*	*10*	*12*	*N · Same*	*GAP (%)*
1500	0	0	0	50	0	0	100	0
2250	0	0	0	44	6	0	100	0
3000	0	0	0	25	9	16	100	0
3750	0	0	0	20	10	20	100	0
4500	0	0	0	15	12	23	100	0
5250	0	0	0	9	8	33	100	0
6000	0	0	0	3	4	43	100	0
6750	0	0	0	1	0	49	100	0
7500	0	0	0	0	1	49	100	0
8250	0	0	0	0	0	50	100	0
9000	0	0	0	0	0	50	100	0

5 Conclusion

In the current work, to solve the routing, modulation format, spatial granularity, and spectrum assignment (RMFSpGlSA) problem, we formulated the ILP model which aims to minimise the overall network cost by reducing the resource (spectrum, WSSs, and lasers) usage in a SDM-b-EON. Initially, we formulated the RMFSpGlSA problem as a joint ILP (J-ILP-RMFSpGlSA) following which, in view of better convergence and obtaining the solutions in reasonable execution times, we split the joint ILP as the RMFSpGl+SA problem (ILP-RMFSpGl+SA). Next, considering two realistic network topologies and parameters, we conducted extensive simulations for evaluating the performances of the two formulated ILP models with an aim to find the 'best' SpGl value under various conditions.

The obtained results demonstrate that when $\sigma_{WSS:FS}$ and $\sigma_{LASER:FS}$ have low values then, compared to the WSSs and the Lasers, there occurs more preservation of the spectrum, and a fine *SpGl* value (e.g., 8) is chosen more number of times compared to a coarse *SpGl* value (e.g., 12) which is always chosen for higher values of $\sigma_{WSS:FS}$ and $\sigma_{LASER:FS}$. Further, a coarse *SpGl* value does not have a major effect on the required FSs amount; however, it significantly impacts the required WSSs and Lasers amount which implies that only when equal importance is imposed on the requirement of all the resources, a coarse *SpGl* value is the 'best' value. It is also observed that the fine values of *SpGl* are mostly chosen with the widening of the guardband width values, and for a guardband width value of 50 GHz, a low *SpGl* value (e.g., 8) is only chosen. Also, the obtained results show that with an increase in the mean bit-rate values of the demands, a coarse value of *SpGl* is mostly chosen. Finally, all the results demonstrate that ILP-RMFSpGl+SA obtains similar performance when compared to J-ILP-RMFSpGlSA simultaneously requiring much lesser execution times.

Owing to the fact that the two formulated ILP models are limited for much larger scale problem instances, as a scope for future research, the author will aim to develop a heuristic algorithm which can be executed in reasonable amounts of times.

References

Christodoulopoulos, K., Tomkos, I. and Varvarigos, E.A. (2011) 'Elastic bandwidth allocation in flexible OFDM based optical networks', *IEEE Journal of Lightwave Technology*, Vol. 29, pp.1354–1366.

Ho, K.P., Kahn, J.M. and Wilde, J.P. (2014) 'Wavelength-selective switches for mode-division multiplexing: scaling and performance analysis', *IEEE Journal of Lightwave Technology*, Vol. 32, pp.3724–3735.

Iyer, S. (2018) 'Traffic grooming with survivability and power-efficiency in software defined elastic optical networks', *Journal of Optics*, Vol. 47, No. 3, pp.351–365.

Iyer, S. (2020) 'An adaptive model for spectrum assignment (ASA) in elastic optical networks', *International Journal of Communication Networks and Distributed Systems*, Vol. 24, No.1, pp.58–82.

Iyer, S. (2020a) 'Investigation of cost and spectrum utilization in internet protocol-over-elastic optical networks', *Journal of Optics*, Vol. 49, No. 3, pp.279–290.

Iyer, S. (2020b) 'An online routing algorithm for space division multiplexing based elastic optical networks', *International Journal of Communication Networks and Distributed Systems*, Vol. 24, No. 2, pp.167–185.

IBM (2020) ILOG CPLEX optimizer. Avalable online at: http://www.ibm.com

Jinno, M. (2017) 'Elastic optical networking: roles and benefits in beyond 100-Gb/s era', *IEEE Journal of Lightwave Technology*, Vol. 35, No. 5, pp.1116–1124.

Khodashenas, P.S., Manuel Rivas-Moscoso, J., Siracusa, D., Pederzolli, F., Shariati, B., Klonidis, D., Salvadori, E. and Tomkos, I. (2017) 'Comparison of spectral and spatial superchannel allocation schemes for SDM networks', *IEEE Journal of Lightwave Technology*, Vol. 34, No. 11, pp.2710–2716.

Klinkowski, M., Lechowicz, P. and Walkowiak, K. (2018) 'Survey of resource allocation schemes and algorithms in spectrally-spatially flexible optical networking', *Optical Switching and Networking*, Vol. 27, No. 1, pp.58–78.

Klonidis, D., Cugini, F., Gerstel, O., Jinno, M., Lopez, V., Palkopoulou, E., Sekiya, M., Siracusa, D., Thouénon, G. and Betouleet, C. (2015) 'Spectrally and spatially flexible optical network planning and operations', *IEEE Communications Magazine*, Vol. 53, No. 2, pp.69–78.

Marom, D.M., Colbourne, P.D., D'errico, A., Fontaine, N.K., Ikuma, Y., Proietti, R., Zong, L., Rivas-Moscoso, J. and Tomkos, I. (2017) 'Survey of photonic switching architectures and technologies in support of spatially and spectrally flexible optical networking', *IEEE/OSA Journal of Optical Communications and Networking*, Vol. 9, pp.1–26.

Marom, D.M. and Blau, M. (2015) 'Switching solutions for WDMSDM optical networks', *IEEE Communications Magazine*, Vol. 53, No. 2, pp.60–68.

Moreno-Muro, F.J., Rumipamba-Zambrano, R., Pavón-Marino, P., Perelló, J., Gené, J.M. and Spadaro, S. (2017) 'Evaluation of core-continuity-constrained ROADMs for Flex-Grid/MCF optical networks', *IEEE/OSA Journal of Optical Communications and Networking*, Vol. 9, No. 11, pp.1041–1050.

Pandya, R.J. (2020) 'Machine learning oriented resource allocation in C+L+S bands extended SDM-EONs', *IET Communications*, Vol. 14, No. 12, pp.1957–1967.

Pandya, R.J. (2020a) 'Survivable virtual topology search with impairment awareness and power economy in optical WDM networks', *International Journal of Communication Networks and Distributed Systems*, Vol. 25, No. 1.

Pandya, R.J., Chandra, V. and Chadha, D. (2014) 'Simultaneous optimization of power economy and impairment awareness by traffic grooming, mixed regeneration, and all-optical wavelength conversion with an experimental demonstration', *IEEE Journal of Lightwave Technology*, Vol. 32, No. 24, pp.4166–4177.

Pandya, R.J., Chandra, V. and Chadha, D. (2014a) 'Impairment-aware routing and wavelength assignment algorithms for optical WDM networks and experimental validation of impairment aware automatic light-path switching', *Optical Switching and Networking*, Vol. 11, No. A, pp.16–28.

Perello, J., Gene, J.M., Pages, A., Lazaro, J.A. and Spadaro, S. (2016) 'Flexgrid/SDM backbone network design with inter-core XT-limited transmission reach', *IEEE/OSA Journal of Optical Communications and Networking*, Vol. 8, pp.540–552.

Rottondi, C., Boffi, P., Martelli, P. and Tornatore, M. (2017) 'Routing, modulation format, baud rate and spectrum allocation in optical metro rings with flexible grid and few-mode transmission', *IEEE Journal of Lightwave Technology*, Vol. 35, No. 1, pp.61–70.

Rumipamba-Zambrano, R., Perelló, J., Gené, J.M. and Spadaro, S. (2018) 'Cost-effective spatial super-channel allocation in Flex-Grid/MCF optical core networks', *Optical Switching and Networking*, Vol. 27, pp.93–101.

Saridis, G.M., Alexandropoulos, D., Zervas, G. and Simeonidou, D. (2015) 'Survey and evaluation of space division multiplexing: From technologies to optical networks', *IEEE Communication Surveys and Tutorials*, Vol. 17, No. 4, pp.2136–2156.

Shariati, B., Rivas-Moscoso, J.M., Marom, D.M., Ben-Ezra, S., Klonidis, D., Velasco, L. and Tomkos, I. (2017) 'Impact of spatial and spectral granularity on the performance of SDM networks based on spatial superchannel switching', *IEEE Journal of Lightwave Technology*, Vol. 35, pp.2559–2568.

Winzer, P.J. and Neilson, D.T. (2017) 'From scaling disparities to integrated parallelism: a decathlon for a decade', *IEEE Journal of Lightwave Technology*, Vol. 35, pp.1099–1115.

Xia, T.J., Fevrier, H., Wang, T. and Morioka, T. (2015) 'Introduction of spectrally and spatially flexible optical networks', *IEEE Communications Magazine*, Vol. 53, pp.24–33.